PHYSICAL REVIEW B VOLUME 48, NUMBER 16 15 OCTOBER 1993-II

Chemical trends and *s*-*p* hybridization in the *DX* center in GaAs

Mineo Saito
NEC Scientific Information System Development, Ltd., 34 Miyukigaoka, Tsukuba, Ibaraki 305, Japan

Atsushi Oshiyama
Microelectronics Research Laboratories, NEC Corporation, 34 Miyukigaoka, Tsukuba, Ibaraki 305, Japan

(Received 25 June 1993)

The Sn- and S-related *DX* centers in GaAs are studied from first-principles calculations based on supercell models within the local-density approximation. The calculated emission barrier for the Sn-related *DX* center with the broken-bond configuration is lower by 0.18 eV than that in Si, in good agreement with the observed value (0.16 eV) from the deep-level transient spectroscopy. This considerably low emission barrier in the Sn-related *DX* center is attributed to weak *s*-*p* hybridization of the Sn dangling bond in the broken-bond configuration. In the case of S, the first-neighbor Ga distorted broken-bond configuration $(\mathrm{Ga_I V_{Ga} S_{As}})^{-1}$ has lower energy than the S-distorted broken-bond configuration $(\mathrm{S_I V_{As}})^{-1}$, and is confirmed to have the lowest energy among the negatively charged geometries. The broken-bond geometry $(\mathrm{Ga_I V_{Ga} S_{As}})^{-1}$ is found to have a surprisingly (0.11 Å) shorter Ga-S bond length than the shallow center. This prominent feature of GaAs:S provides important insight for the explanation of results of an extended x-ray-absorption fine-structure measurement. Finally, we reveal that the chemical trend in the stability of the broken-bond geometries of the *DX* center is closely related to the degree of the *s*-*p* hybridization inherent to the distorted atom.

I. INTRODUCTION

In *n*-type $\mathrm{Al}_x\mathrm{Ga}_{1-x}\mathrm{As}$ and GaAs, bistability between the shallow center with the typical effective-mass state, and the *DX* center with a localized electronic state has been observed: the two centers originate from a donor impurity (Si, Ge, Sn, S, Se, or Te) alone and correspond to geometries different from each other.[1] The *DX* center becomes stabler than the shallow one when $x \geq 0.22$ or when pressure is applied to GaAs, and then shows physically interesting properties:[2] it has barriers for both electron emission and capture, leading to persistent photoconductivity; there is a large Stokes shift between thermal and optical ionization energies.

Some models are proposed for the *DX* center with the above-mentioned features.[3-12] Among them two models are proposed on the basis of first-principles calculations: a neutral on-site model[11] and a negative broken-bond model.[12] In the latter model proposed by Chadi and Chang,[12] the impurity atom (the nearest-neighbor Ga atom) is displaced along the $[\bar{1}\,\bar{1}\,\bar{1}]$ axis and a σ bond is broken in the case of group-IV (group-VI) impurity atoms. This model for Si is denoted by $(\mathrm{Si_I\,V_{Ga}})^{-1}$, which means that Si is at an interstitial site and the substitutional Ga site is vacant. There is a controversy[11-17] on the total-energy difference between the neutral and negative on-site geometries and the negative broken-bond one. As for the Si-related *DX* center, however, an accumulation of theoretical studies[12,15-20] reveals that the broken-bond model is consistent with various experimental results.

Recently, Saito, Oshiyama, and Sugino[17,18] emphasized that, in the *DX* center with the stable broken-bond geometry, the position of the Si atom on the $[\bar{1}\,\bar{1}\,\bar{1}]$ axis passes the sp^2 hybridization point, where the Si-As bond angle is 120° (see Fig. 1). This peculiar atomic configuration is referred to as $sp^{2+\alpha}$ hybridization configuration, where α is deduced from the Si-As bond angle (θ) as $2+\alpha=-1/\cos\theta$ (Ref. 21). In the case of Si, α is found to be 0.4 since $\theta=115°$. The energy gain by the variation from the sp^2 hybridization to $sp^{2+\alpha}$ hybridization structures stabilizes the broken-bond configuration and *the value of α is thus a criterion of stability of the broken-bond configuration.*

In comparison with the Si-related *DX* center, theoretical study on other elements is insufficient. In this paper, we thus investigate the Sn-related and S-related *DX* centers and compare the results with those for Si. Important findings in this study are as follows. In the case of Sn, distortion of the Sn atom in the stable broken-bond configuration is smaller than that for Si by 0.08 Å, and $\alpha=0.2$ in contrast with $\alpha=0.4$ in Si. Because of the small value of α, the calculated electron emission barrier is considerably lower by 0.18 eV than that of Si, in good

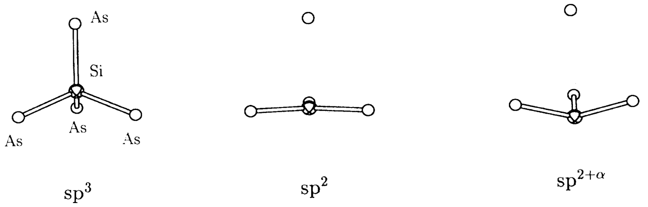

FIG. 1. Three typical *s*-*p* hybridization structures for GaAs:Si. In the on-site geometry, the hybridization is sp^3, and, in the stable broken-bond geometry (*DX* center), the hybridization is $sp^{2+\alpha}$.

agreement with an experimental value (0.16 eV). In $(\mathrm{Ga_I V_{Ga} S_{As}})^{-1}$, in which a first-nearest-neighbor Ga atom is distorted along the $[\bar{1}\bar{1}\bar{1}]$ axis, α equals 0.5 for the Ga atom, while in the metastable S-distorted broken-bond configuration $(\mathrm{S_I V_{As}})^{-1}$, α for the S atom is surprisingly small (0.0). As a result, the former configuration for the *DX* center has 0.21-eV lower energy than the latter one and is confirmed to have the lowest energy among the negatively charged configurations. The shallow center is found to have a considerably (0.11 Å) longer Ga-S bond length than the *DX* center $(\mathrm{Ga_I V_{Ga} S}_{As})^{-1}$. This prominent feature of the S-related *DX* center provides important insights for the explanation of experimental results from an extended x-ray-absorption fine-structure (EXAFS) measurement.

II. METHOD

Since the details of the calculational method have been reported in a previous study,[17] we give here a brief description of the outline. Supercell calculations are performed by applying the norm-conserving pseudopotential method[22] within the local-density approximation. The cell contains 32 or 64 sites and the cutoff energy for the plane waves is 8–12 Ry. The number of the sampling k points in the Brillouin zone is taken to be 4 by following Baldereschi.[23] In order to perform large-scale calculations, we employ the conjugate-gradient method[24] with separable forms of the pseudopotentials. Since the separable potential proposed by Kleinman-Bylander[25]does not give reliable results for the s part of the pseudopotentials of the Ga and As atoms, the real-space partitioned separable pseudopotential[26] is used for these atoms. We have examined reliability of the pseudopotentials by performing various calculations.[17,18] In this paper, reliability of the S pseudopotential is newly examined by performing total-energy calculation for the SiS molecule: in the supercell calculation, the SiS molecule is located in each cubic cell with the side length of 20 a.u. The optimized bond lengths are 1.931, 1.937, 1.940, and 1.940 Å for the 8-, 10-, 12-, and 16-Ry cutoff energies, respectively, and these values are consistent with the experimental one (1.929 Å) within the deviation of 0.6%. In the geometry optimization of GaAs:Sn and GaAs:S, we relax all the atoms in the unit cell in order to include the medium-range relaxation.

III. RESULTS AND DISCUSSION

In this section we present results for Sn- and S-related *DX* centers. The broken-bond geometry is discussed in terms of the s-p hybridization in the dangling bond of the distorted atom.

A. Sn-related *DX* center

First, we report the results of the Sn-related *DX* center with the broken-bond geometry. The calculation is performed by using the 64-site cell with the cutoff energy of 8 Ry. In the optimized geometry, the displacement of the Sn atom along the $[\bar{1}\bar{1}\bar{1}]$ axis is 1.29 Å and the Sn-As σ bond length is 2.60 Å, which is longer by 0.15 Å than the crystal bond length (2.45 Å). The Sn-As bond angle (117°) is slightly smaller than the sp^2 hybridization angle (120°) and $\alpha=0.2$ is deduced from this angle. Relation between α and s-p hybridization in the nonbonding orbital of a threefold-coordinated atom is shown in Fig. 2: When $\alpha=0$ (the bond angle is 120°), there is no s-p hybridization in the nonbonding orbital, i.e., the orbital has the p_π character; as α becomes large (as the bond angle becomes smaller than 120°), the s component in the nonbonding orbital increases, and as a result the orbital has an s-p hybridized dangling-bond character. Thus the optimized nonzero value of $\alpha(0.2)$ in the stable broken-bond geometry indicates that the Sn atom has an s-p hybridized dangling bond: indeed, as shown in Fig. 3, the Sn atom has the dangling bond in the $[\bar{1}\bar{1}\bar{1}]$ direction. It should be noticed that the energy level of this dangling bond is lowered by inclusion of the Sn s orbital. This inclusion of the s component is the origin of the energy gain related to the variation from the sp^2 hybridization to the $sp^{2+\alpha}$ hybridization structures. Thus we expect that broken-bond geometry with large α is generally stable, since large α is accompanied with a large amount of s component in the dangling bond. The remaining threefold As atom moves by 0.13 Å along the $[\bar{1}\bar{1}\bar{1}]$ axis and this *inward* motion of the As atom toward the Sn atom makes the Ga-As bond angle (106°) less than the tetrahedral angle(109.5°). We emphasize that this reduction of the Ga-As bond angle lowers the As dangling-bond energy by increasing the s component of the dangling bond (see Fig. 2) and thus, in addition to the energy gain from the s-p hybridization in the Sn dangling bond, stabilizes the broken-bond geometry.

We now compare the broken-bond geometry of the Sn-related *DX* center with that of the Si-related *DX* center which has been obtained from the supercell calculation with the same size.[17] The displacement (1.37 Å) of the Si atom along the $[\bar{1}\bar{1}\bar{1}]$ is larger by 0.08 Å and thus

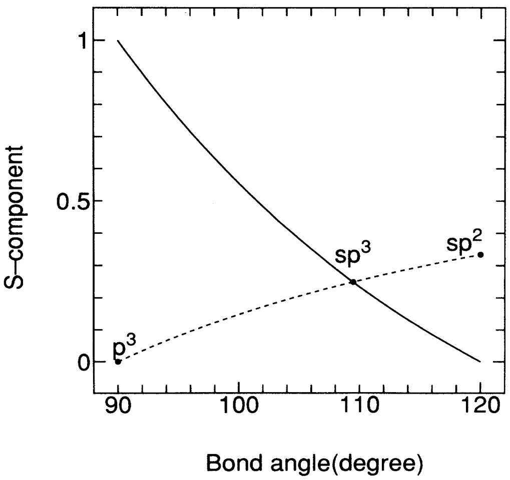

FIG. 2. The ratio of the s component in the one nonbonding orbital (solid line) and the three σ bond orbitals (dashed line) for a threefold-coordinated atom as a function of the bond angle. The values of the ratio are obtained from the orthogonal condition for the hybridized orbitals (Ref. 17).

$\alpha(0.4)$ is larger by 0.2, compared with the case of Sn. The small value of α in Sn indicates that s-p hybridization in the Sn dangling bond is weak, i.e., the s component of the dangling bond is small. Indeed the weak s-p hybridization is a general feature for the Sn atom: While Si forms a stable diamond (sp^3 hybridization) structure at room temperature, Sn forms a metallic β-tin(very weak s-p hybridization) structure at the same temperature. The difference between Si and Sn is due to the fact that the s-p promotion of electrons is suppressed as the covalent radius becomes large. It was previously found[18] for the Ge-related DX center that the displacement of the Ge atom along the $[\bar{1}\,\bar{1}\,\bar{1}]$ axis is smaller by only 0.01 Å than that in Si and the value of α is thus identical to that in Si. The similar broken-bond geometries between Ge and Si are reasonable since the second-row and third-row atoms have relatively similar chemical properties.

The small value of α in Sn suggests that the broken-bond geometry is not very stable compared with the case of Si. The Sn-related DX center is thus expected to have a low electron emission barrier, which is located between the stable broken-bond and the on-site geometries. In order to confirm this expectation, we calculate the electron emission barrier by using the 32-site cell with 12-Ry cutoff energy. In the geometry optimization for the stable broken-bond and transition geometries under the zero pressure, we relax all atoms in the unit cell except for six boundary Ga atoms.[27] In the transition states, the Sn and Si atoms are distorted from the substitutional site by 0.46 and 0.55 Å along the $[\bar{1}\,\bar{1}\,\bar{1}]$ axis, respectively, and the calculated barriers for Sn and Si are 0.17 and 0.35 eV, respectively. We therefore conclude that the emission barrier of the Sn-related DX center is much (0.18 eV) lower than that of the Si-related DX center. It is found that the pressure dependence of the emission barrier is quite small: under the high pressure of 28 kbar, the calculated emission barriers of Si and Sn are 0.15 and 0.33 eV, respectively, and thus the difference in the barrier between Sn and Si is 0.18 eV. The observed emission barriers from the deep-level transient spectroscopy (DLTS) measurements[28] under the high pressure of 28 kbar are 0.32 and 0.16 eV for Si and Sn. Therefore the calculated difference in the emission barrier (0.18 eV) between Sn and Si is consistent with the experimental value (0.16 eV).

We next discuss an effect of local atomic configurations in $Al_xGa_{1-x}As$:Sn, compared with the case of $Al_xGa_{1-x}As$:Si. DLTS measurements[29–31] and first-principles calculation[20] suggest that the electron emission barrier of the Si-related DX center increases by about 0.1 eV through Al substitution for the second nearest Ga sites around the Si atom. The increase of the emission barrier is expected to be due to the fact that the interaction between the Si dangling bond and the Al atom at the second nearest site lowers the total energy of the broken-bond configuration.[20] We speculate that this effect of the local atomic configuration is weak in the case of Sn for the following reasons. First, the present calculation (64-site cell model with the 8-Ry cutoff energy) shows that the distance between the Sn and the second nearest Ga atoms (3.09 Å) is longer than that in the case of Si (2.98 Å), suggesting that the interaction between the Sn dangling bond and the second nearest atoms is weak. Second, the Sn dangling-bond charge density shown in Fig. 3 is found to be lower than that in Si. This low dangling-bond charge density contributes to the weak interaction with the second nearest atoms.

Finally, total energies of several negatively charged geometries of the Sn impurity are evaluated by using the 32-site cell model with the 12-Ry cutoff energy. The energy of the negatively charged on-site geometry, D^{-1}, has higher energy than that of the broken-bond geometry by 0.16 eV. This energy difference is smaller than the corresponding value for Si (0.25 eV). One of the reasons is the small value of α in the Sn-related DX center. The metastable structure $(\mathrm{Sn_{Ga}As_I V_{As}})^{-1}$, in which the nearest As atom is distorted along the [111] axis and becomes threefold coordinated, was recently found by Chadi.[16] The present calculation shows that the geometry has 0.16 eV higher energy than the Sn-distorted broken-bond geometry. We therefore conclude that the broken-bond

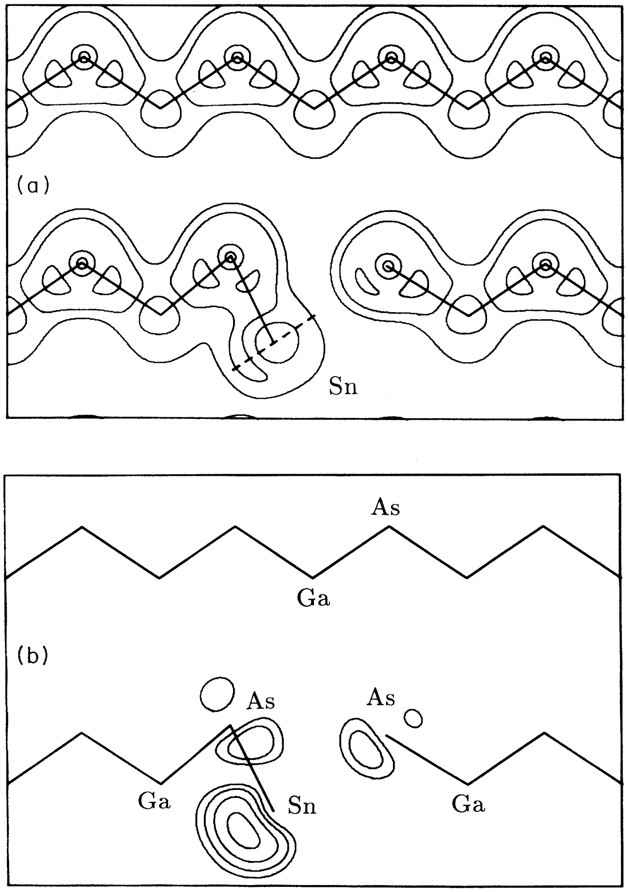

FIG. 3. (a) The total electron density on the $(1\bar{1}0)$ plane of the Sn-related DX center. The values of the contour lines are 0.08×2^n $e/(\mathrm{a.u.})^3$, where $n=0$, 1, or 2. The dashed line indicates the [111] axis. (b) The electron charge density on the $(1\bar{1}0)$ plane for the gap level of the Sn-related DX center. The values of the contour lines are 0.04×2^n $e/(\mathrm{a.u.})^3$, where $n=0$, 1, 2, or 3.

geometry $(\mathrm{Sn_I V_{Ga}})^{-1}$ has the lowest energy among the negatively charged geometries.

B. S-related *DX* center

We study GaAs:S by using the 64-site cell model. First, we optimize the geometry of the shallow state, d^0, with the 10-Ry cutoff energy. Since the wave function of the shallow level is considerably delocalized, the electron occupying the level has a negligibly small effect on the atomic geometry. Thus the actual calculation is performed for the positive state d^+ with the on-site geometry. In the optimized geometry, the Ga-S bond length is 2.51 Å, which is longer by 0.06 Å than the crystal bond length. Since the *s* level of S is lower than that in As, the S *s* bonding level becomes a hyperdeep level, which is 1.0 eV lower than the valence-band bottom. The charge density for this state (Fig. 4) shows that the electrons are highly localized around the S atom.

Using the 10-Ry cutoff energy, we optimize the Ga-distorted broken-bond geometry $(\mathrm{Ga_I V_{Ga} S_{As}})^{-1}$, in which the first-neighbor Ga atom is displaced along the $[\bar{1}\bar{1}\bar{1}]$ axis. The amount of the displacement of the Ga atom is 1.44 Å and the Ga-As bond length (2.45 Å) is identical to the crystal bond length. This distortion of Ga induces a large value (0.5) of α, and thus stabilizes the Ga dangling bond in the $[\bar{1}\bar{1}\bar{1}]$ direction (see Fig. 5). The remaining threefold-coordinated S atom is displaced along the [111] axis by 0.09 Å and this *outward* motion of the S atom in the opposite direction of the distorted Ga atom increases the Ga-S bond angle (111°) from the tetrahedral one. This *outward* motion of S is in contrast with the *inward* motion which was found in the threefold-coordinated As atom of the Sn-related *DX* center. As was mentioned, in the case of $(\mathrm{Sn_I V_{Ga}})^{-1}$, the As *inward* motion with the reduction of the Ga-As bond angle stabilizes the As dangling bond by increasing the *s* component of the dangling bond. In $(\mathrm{Ga_I V_{Ga} S_{As}})^{-1}$, however, the *inward* motion of the S atom with the reduction of the Ga-S bond angle does not stabilize the S dangling bond because the increase of the *s* component in the dangling bond is prevented from the weak *s-p* hybridization character in the S atom. This character of the S atom is due to its deep *s* level. Indeed, an extremely weak *s-p* hybridization feature of the S nonbonding orbital can be seen in Fig. 5: The total electron density around the S atom is surprisingly almost symmetric along the [111] axis, indicating that the nonbonding orbital of the S atom mainly consists of the $p_{[\bar{1}\bar{1}\bar{1}]}$ orbital and thus the *s* component in the nonbonding orbital is very small. Figure 2 suggests that the theoretically discovered *outward* motion of the S atom which causes the increase of the Ga-S bond angle (111°) increases the *s* component for the Ga-S σ bond and thus stabilizes the bond. It is found that the Ga-S σ bond charge increases compared with that in d^+ (see Figs. 4 and 5). It is thus reasonable that the optimized Ga-S bond length (2.40 Å) is much (0.11 Å) shorter than that of d^+ (2.51 Å). This peculiar feature of the S-related *DX* center is in contrast with those for the *DX* centers related to the group-IV atoms (Si, Ge, and Sn): in a previous work,[18] it was found that the distances between the impurity and the nearest As atoms in the d^+

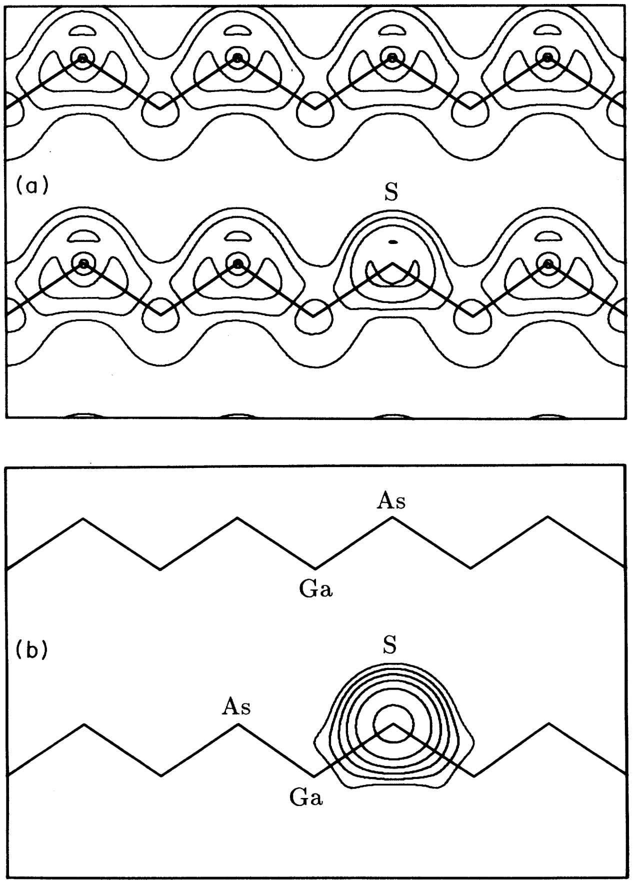

FIG. 4. (a) The total electron density on the (1$\bar{1}$0) plane of the on-site geometry, d^+ of GaAs:S. The values of the contour lines are 0.142×2^n $e/(\mathrm{a.u.})^3$, where $n=0$, 1, 2, or 3. (b) The electron density on the (1$\bar{1}$0) plane for the hyperdeep level, which is located 1.0 eV below the valence-band bottom. The values of the contour lines are 0.08×2^n $e/(\mathrm{a.u.})^3$, where $n=0$, 1, 2, 3, 4, or 5.

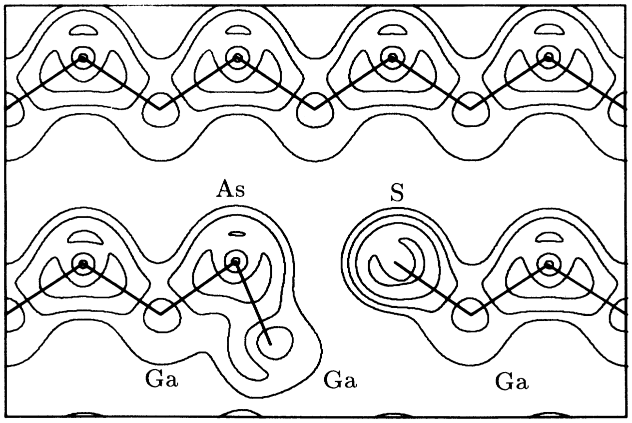

FIG. 5. The total electron density on the (1$\bar{1}$0) plane of the S-related *DX* center, $(\mathrm{Ga_I V_{Ga} S_{As}})^{-1}$. The value of the contour lines are the same as Fig. 4(a).

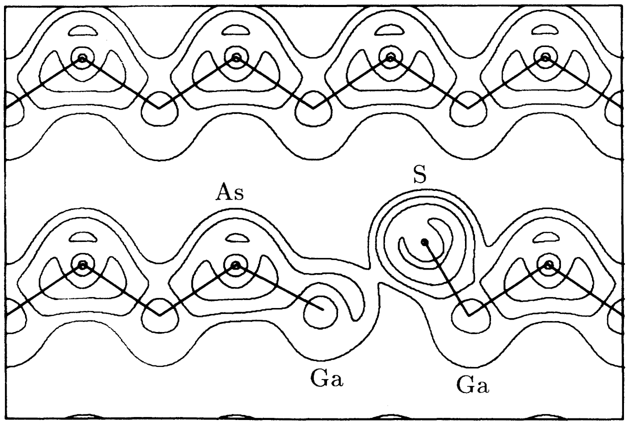

FIG. 6. The total electron density on the $(1\bar{1}0)$ plane of the metastable S-distorted broken-bond geometry, $(S_I V_{As})^{-1}$. The values of the contour lines are the same as Fig. 4(a).

and *DX* centers are very close to each other.

The total energies for several negatively charged geometries of the S impurity are compared by performing the calculation with the 8-Ry cutoff energy.[32] The total energy of the Ga-distorted broken-bond geometry $(Ga_I V_{Ga} S_{As})^{-1}$ is lower by 0.13 eV than that of D^{-1} and lower by 0.21 eV than that of the S-distorted broken-bond geometry $(S_I V_{As})^{-1}$. It is thus confirmed that the Ga-distorted broken-bond geometry $(Ga_I V_{Ga} S_{As})^{-1}$ has the lowest energy among the negatively charged geometries. In the metastable S-distorted broken-bond geometry $(S_I V_{As})^{-1}$, the threefold-coordinated Ga atom is displaced by 0.30 Å along the [111] axis and this *inward* motion toward the S atom makes the Ga-As bond angle (101°) less than the tetrahedral angle. The Ga dangling bond in the [111] direction (see Fig. 6) is thus stabilized by the increase of the *s* component. The optimized Ga-As bond length is 2.56 Å, which is much (0.11 Å) longer than the crystal bond length. The displacement of the S atom in the S-distorted broken-bond geometry is small (1.06 Å) compared with the corresponding value (1.44 Å) of the first nearest Ga atom in the Ga-distorted broken-bond geometry, and thus α (0) of the S atom in the S-distorted broken-bond geometry is very small.[33] This small value of α is due to the weak *s*-*p* hybridization character of the S atom. It is emphasized that the surprisingly small value of α is the reason for the metastability of $(S_I V_{As})^{-1}$: The total energy is higher than that of the most stable Ga-distorted broken-bond geometry.

Finally, as was mentioned, the present calculation shows that the *DX* center with the Ga-distorted broken-bond geometry $(Ga_I V_{Ga} S_{As})^{-1}$ has a much (0.11 Å) shorter Ga-S bond length than d^+. Thus, if the reaction $2d^0 \rightarrow d^+ + DX^{-1}$ occurs, two nearest-neighbor peaks corresponding to the short bond length of DX^{-1} and the long bond length of d^+ would be detected by an EXAFS measurement. Actually by performing an EXAFS study[34] on S implanted in GaAs, Sette *et al.* detected an abnormally broad first-nearest-neighbor peak: The broad peak is expected to be due to the above-mentioned two impurities (d^+ and DX^{-1}) with different Ga-S bond lengths. The observed distance (2.33±0.03 Å) of the broad peak is, however, slightly smaller than the calculated smaller length (2.40 Å) of the Ga-S bond (DX^{-1} has the shorter bond). Since the energy of the *s* orbital of S is proximate to that of the 3*d* core orbital of Ga, the interaction between these orbitals might shorten the Ga-S bond length: In the present pseudopotential calculation, the 3*d* core orbital is frozen. To the contrary, Sette *et al.* considered from their analysis on the experimental results that the detected abnormally broad peak is due to the substitutional S impurity, S_{As}, with the bond length of 2.43±0.04 Å and the complex $S_{As} V_{As'}$ of the As vacancy and the substitutional S impurity with the bond length of 2.31±0.04 Å. The former Ga-S bond length is close to the calculated bond length of the substitutional geometry (2.51 Å), but it is not clear whether the complex $S_{As} V_{As'}$, has the much shorter Ga-S bond length.

IV. CONCLUSION

We have studied the Sn- and S-related *DX* centers by performing first-principles supercell calculations within the local-density approximation. The value of α deduced from the optimized geometry of the Sn-related *DX* center is 0.2 in contrast with 0.4 in the Si-related *DX* center. This smaller value of α is due to the fact that the *s*-*p* hybridization of Sn is weaker than that of Si. As a result, the calculated emission barrier for the Sn-related *DX* center is much (0.18 eV) lower than that for the Si-related *DX* center. The value of α of a first neighbor Ga atom is 0.5 for the S-related *DX* center $(Ga_I V_{Ga} S_{As})^{-1}$, while in the S-distorted broken-bond geometry $(S_I V_{As})^{-1}$, $\alpha = 0.0$ for the distorted S atom. This surprisingly small value of α is due to the fact that the S atom has very weak *s*-*p* hybridization character. Thus $(Ga_I V_{Ga} S_{As})^{-1}$ with the large value of α has 0.21 eV lower energy than $(S_I V_{As})^{-1}$, which has the small value of α. $(Ga_I V_{Ga} S_{As})^{-1}$ is confirmed to have the lowest total energy among the negatively charged geometries. Finally, the *DX* center $(Ga_I V_{Ga} S_{As})^{-1}$ is found to have a much (0.11 Å) shorter Ga-S bond length than d^+. This prominent difference in the Ga-S bond length, which we have found, is consistent with results from an EXAFS study by Sette *et al.*

Finally, it is expected from present calculational results that the distorted atom with strong *s*-*p* hybridization tends to form a stable broken-bond geometry with large α. In the case of the group-IV atom (Si, Ge, and Sn) related *DX* center, the value of α increases as the atom becomes lighter. In the case of the group-VI atom (S, Se, and Te), it is expected that the impurity atom distorted broken-bond configurations have a very small value of α since the group-VI atoms have a weak *s*-*p* hybridization character. The group-VI atom distorted broken-bond configurations are thus expected to have higher energy than the first nearest Ga atom distorted broken-bond configurations.

ACKNOWLEDGMENTS

We thank Dr. O. Sugino, Dr. Y. Mochizuki, and Dr. Y. Miyamoto for fruitful discussions.

[1] For a review, see T. N. Theis, in *Proceedings of the Fourteenth International Symposium on Gallium Arsenide and Related Compounds,* edited by A. Christou and H. S. Rupprecht, IOP Conf. Proc. No. 91 (Institute of Physics and Physical Society, London, 1990), p. 1; M. Mizuta, in *Proceedings of International Conference on Science and Technology of Defect Control in Semiconductors, Yokohama, Japan,* edited by K. Sumino (Elsevier, Amsterdam, 1990), p. 1043; P. M. Mooney, J. Appl. Phys. **67**, R1 (1990); Semicond. Sci. Technol. **6**, B1(1991).

[2] D. V. Lang and R. A. Logan, Phys. Rev. Lett. **39**, 635 (1977); D. V. Lang, R. A. Logan, and M. Jaros, Phys. Rev. B **19**, 1015 (1979).

[3] A. K. Saxena, Solid-State Electron. **25**, 127 (1982).

[4] T. N. Morgan, Phys. Rev. B **34**, 2664 (1986).

[5] A. Oshiyama and S. Ohnishi, Phys. Rev. B **33**, 4320 (1986).

[6] P. M. Mooney, G. A. Northrop, T. N. Morgan, and H. G. Grimmeiss, Phys. Rev. B **37**, 8298 (1988).

[7] H. P. Hjalmarsom and T. J. Drummond, Phys. Rev. Lett. **60**, 2410 (1988).

[8] J. C. Bourgoin, S. L. Feng, and H. J. von Bardeleben, Phys. Rev. B **40**, 7663 (1989).

[9] Y. Mochizuki, M. Mizuta, and A. Oshiyama, Jpn. J. Appl. Phys. **29**, L530 (1990).

[10] T. N. Morgan, Semicond. Sci. Technol. **6**, B23 (1991).

[11] E. Yamaguchi, K. Shiraishi, and T. Ohno, J. Phys. Soc. Jpn. **60**, 3093 (1991); in *Proceedings of the 20th International Conference on the Physics of Semiconductors, Thessaloniki, Greece, 1990,* edited by E. M. Anastassakis and J. D. Joannopoulos (World Scientific, Singapore, 1990), p. 501.

[12] D. J. Chadi and K. J. Chang, Phys. Rev. Lett. **61**, 873 (1988); Phys. Rev. B **39**, 10 063 (1989).

[13] R. Jones and S. Öberg, Phys. Rev. B **44**, 3407 (1991).

[14] T. Ohno and E. Yamaguchi, Phys. Rev. B **44**, 6527 (1991).

[15] J. Dabrowski, M. Scheffler, and R. Strehlow, in *Proceedings of the 20th International Conference on the Physics of Semiconductors* (Ref. 11), p. 489.

[16] D. J. Chadi, Phys. Rev. B **46**, 6777 (1992).

[17] M. Saito, A. Oshiyama, and O. Sugino, Phys. Rev. B **47**, 13 205 (1993).

[18] M. Saito, A. Oshiyama, and O. Sugino, Phys. Rev. B **45**, 13 745 (1992).

[19] S. B. Zhang and D. J. Chadi, Phys. Rev. B **42**, 7174 (1990).

[20] S. B. Zhang, Phys. Rev. B **44**, 3417 (1991).

[21] The expression is derived from the orthogonal condition for the hybridized orbital (see the Appendix in Ref. 17).

[22] A. Oshiyama and M. Saito, J. Phys. Soc. Jpn. **56**, 2104 (1987); Phys. Rev. B **36**, 6156 (1987).

[23] A. Baldereschi, Phys. Rev. B **7**, 5212 (1973).

[24] O. Sugino and A. Oshiyama, in *Proceedings of the 16th International Conference on Defects in Semiconductors, Lehigh, 1991,* edited by G. Davies, G. G. Deleo, and M. Stavola (Trans Tech, Aedermannsdorf, Switzerland, 1991), p. 469.

[25] L. Kleinman and D. M. Bylander, Phys. Rev. Lett. **48**, 1425 (1982).

[26] M. Saito, O. Sugino, and A. Oshiyama, Phys. Rev. B **46**, 2606 (1992).

[27] This restriction raises the energy of the Sn broken-bond geometry by 0.04 eV compared with the case of the full optimization.

[28] T. Fujisawa, J. Yoshino, and H. Kukimoto, J. Cryst. Growth **98**, 243 (1989).

[29] P. M. Mooney, T. N. Theis, and S. L. Wright, Appl. Phys. Lett. **53**, 2546 (1988).

[30] T. Baba, M. Mizuta, T. Fujisawa, J. Yoshino, and H. Kukimoto, Jpn. J. Appl. Phys. **28**, L891 (1989).

[31] L. Dobaczewski, P. Kaczor, M. Missous, A. R. Peaker, and Z. R. Żytkiewicz, Phys. Rev. Lett. **68**, 2508 (1992).

[32] The calculation with the 8-Ry cutoff energy gives deviation for the optimized bond lengths within 0.8% from the values of the calculation with the 10-Ry cutoff energy.

[33] The Ga-S bond angle and length are 119.5° and 2.37 Å, respectively.

[34] F. Sette, S. J. Pearton, J. M. Poate, and J. E. Rowe, Phys. Rev. Lett. **56**, 2637 (1986).